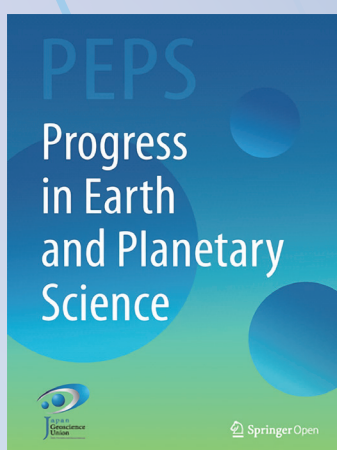


The collection of review articles

Progress in Earth and Planetary Science

(the 1st edition: published from April 2014 to January 2021)



Japan Geoscience Union (JpGU) Open Access journal

<https://progearthplanetsci.springeropen.com/>



CONTENTS

1. Space and planetary sciences

Review of the accomplishments of Mid-latitude Super Dual Auroral Radar Network (SuperDARN)	
HF Radars	2
Scientific innovations from the Mars aerosol optical depth based on satellite data with a temporal resolution of hours	3
Simulation study of near-Earth space disturbances: 1. Magnetic storms	4
Simulation study of near-Earth space disturbances: 2. Auroral substorms	5
Day-to-day and short-term variabilities in the equatorial plasma bubble/spread F irregularity seeding and development	6
Asteroid Ryugu before the Hayabusa2 encounter	7
Review of the generation mechanisms of post-midnight irregularities in the equatorial and low-latitude ionosphere	8
Lightning detection on Venus: a critical review	9
Post-sunset rise of equatorial <i>F</i> layer—or upwelling growth?	10
Effects of the postsunset vertical plasma drift on the generation of equatorial spread F	11
A review on the numerical simulation of equatorial plasma bubbles toward scintillation evaluation and forecasting	12
Mars core structure — concise review and anticipated insights from InSight	13
Extreme geomagnetically induced currents	14
Magnetohydrodynamics Modeling of Coronal Magnetic Field and Solar Eruptions Based on the Photospheric Magnetic Field	15
MF and HF radar techniques for investigating the dynamics and structure of the 50 to 110 km height region: a review	16
Advancing the understanding of the Sun-Earth interaction - the Climate and Weather of the Sun-Earth System (CAWSES) II Program	17
The science case for the EISCAT_3D radar	18
Short-term variability of the Sun-Earth system: an overview of progress made during the CAWSES-II period	19
eScience and Informatics for International Science Programs	20
What is the solar influence on climate? Overview of activities during CAWSES-II	21
Response of the mesosphere-thermosphere-ionosphere system to global change – CAWSES-II contribution	22
The geospace response to variable inputs from the lower atmosphere: A review of the progress made by Task Group 4 of CAWSES-II	23

2. Atmospheric and hydrospheric sciences

Marine microplastics as vectors of major ocean pollutants and its hazards to the marine ecosystem and humans	26
Applications of soft computing models for predicting sea surface temperature: a comprehensive review and assessment	27
Two decades of Earth system modeling with an emphasis on Model for Interdisciplinary Research on Climate (MIROC)	28
d4PDF: large-ensemble and high-resolution climate simulations for global warming risk assessment	29

DYAMOND: The DYNAMics of the Atmospheric general circulation Modeled On Non-hydrostatic Domains ...	30
Toward reduction of the uncertainties in climate sensitivity due to cloud processes using a global non-hydrostatic atmospheric model	31
Maritime continent coastlines controlling Earth's climate	32
Outcomes and challenges of global high-resolution non-hydrostatic atmospheric simulations using the K computer	33
A review of atmospheric chemistry observation at mountain sites	34
A review of progress towards understanding the transient global mean surface temperature response to radiative perturbation	35
Overview of the development of the Aerosol Loading Interface for Cloud microphysics In Simulation (ALICIS)	36
The dynamics of the mesosphere and lower thermosphere: a brief review	37
Modeling in Earth system science up to and beyond IPCC AR5	38
The Non-hydrostatic Icosahedral Atmospheric Model: Description and Development	39

3. Human geosciences • Biogeosciences

Arsenic cycling in the Earth's crust and hydrosphere: interaction between naturally occurring arsenic and human activities	42
Perspective on the response of marine calcifiers to global warming and ocean acidification – Behavior of corals and foraminifera in a high CO ₂ world “hot house”	43
Theoretical constraints of physical and chemical properties of hydrothermal fluids on variations in chemolithotrophic microbial communities in seafloor hydrothermal systems.	44
Biochemical and physiological bases for the use of carbon and nitrogen isotopes in environmental and ecological studies	45

4. Solid earth sciences

Visualizing heterogeneities of earthquake hypocenter catalogs: modeling, analysis, and compensation	48
Strength models of the terrestrial planets and implications for their lithospheric structure and evolution	49
Deep mantle melting, global water circulation and its implications for the stability of the ocean mass	50
A coupled core-mantle evolution: Review and future prospects	51
Some remarks on hydrogen-assisted electrical conductivity in olivine and other minerals	52
Detection of repeating earthquakes and their application in characterizing slow fault slip	53
Nitrogen in the Earth: abundance and transport	54
Earthquake Early Warning: what does “seconds before a strong hit” mean?	55
Redox-controlled mechanisms of C and H isotope fractionation between silicate melt and COH fluid in the Earth's interior	56
Nonlinear dynamical analysis of GNSS data: quantification, precursors and synchronization	57
Structural context and variation of ocean plate stratigraphy, Franciscan Complex, California: insight into mélange origins and subduction-accretion processes	58
Seismic imaging of slab metamorphism and genesis of intermediate-depth intraslab earthquakes	59
Imaging in 3D under pressure: a decade of high-pressure X-ray microtomography development at GSECARS	60
Philippine Sea Plate inception, evolution and consumption with special emphasis on the early stages of Izu-Bonin-Mariana subduction	61
Mantle hydration and Cl-rich fluids in the subduction forearc	62

Iron snow, crystal floats, and inner-core growth: modes of core solidification and implications for dynamos in terrestrial planets and moons	63
Liquid Sodium Models of the Earth's Core	64
Towards more realistic core-mantle boundary heat flux patterns: a source of diversity in planetary dynamos	65
Sound velocity of hcp-Fe at high pressure: experimental constraints, extrapolations and comparison with seismic models	66
Earthquake faulting in subduction zones: insights from fault rocks in accretionary prisms	67
Water-melt interaction in hydrous magmatic systems at high temperature and pressure	68

5. Interdisciplinary research

Coupling library Jcup3: its philosophy and application	70
Morphometric measurements of bedrock rivers at different spatial scales and applications to geomorphological heritage research	71
Northern Eurasia Future Initiative (NEFI): facing the challenges and pathways of global change in the twenty-first century	72
Cenozoic sedimentary records of climate-tectonic coupling in the Western Himalaya	73
Transitional changes in microfossil assemblages in the Japan Sea from the Late Pliocene to Early Pleistocene related to global climatic and local tectonic events	74
Evolution and variability of the Asian monsoon and its potential linkage with uplift of the Himalaya and Tibetan Plateau	75
Geochemical approaches to the quantification of dispersed volcanic ash in marine sediment	76
Sea surface temperature proxies (alkenones, foraminiferal Mg/Ca, and planktonic foraminiferal assemblage) and their implications in the Okinawa Trough	77
Marine tephra in the Japan Sea sediments as a tool for paleoceanography and paleoclimatology	78
The Pliocene to Recent History of the Kuroshio and Tsushima Currents: a multi-proxy approach	79

CONTENTS

1. Space and planetary sciences

Review of the accomplishments of Mid-latitude Super Dual Auroral Radar Network (SuperDARN)	
HF Radars	2
Scientific innovations from the Mars aerosol optical depth based on satellite data with a temporal resolution of hours	3
Simulation study of near-Earth space disturbances: 1. Magnetic storms	4
Simulation study of near-Earth space disturbances: 2. Auroral substorms	5
Day-to-day and short-term variabilities in the equatorial plasma bubble/spread F irregularity seeding and development	6
Asteroid Ryugu before the Hayabusa2 encounter	7
Review of the generation mechanisms of post-midnight irregularities in the equatorial and low-latitude ionosphere	8
Lightning detection on Venus: a critical review	9
Post-sunset rise of equatorial <i>F</i> layer—or upwelling growth?	10
Effects of the postsunset vertical plasma drift on the generation of equatorial spread F	11
A review on the numerical simulation of equatorial plasma bubbles toward scintillation evaluation and forecasting	12
Mars core structure — concise review and anticipated insights from InSight	13
Extreme geomagnetically induced currents	14
Magnetohydrodynamics Modeling of Coronal Magnetic Field and Solar Eruptions Based on the Photospheric Magnetic Field	15
MF and HF radar techniques for investigating the dynamics and structure of the 50 to 110 km height region: a review	16
Advancing the understanding of the Sun-Earth interaction - the Climate and Weather of the Sun-Earth System (CAWSES) II Program	17
The science case for the EISCAT_3D radar	18
Short-term variability of the Sun-Earth system: an overview of progress made during the CAWSES-II period	19
eScience and Informatics for International Science Programs	20
What is the solar influence on climate? Overview of activities during CAWSES-II	21
Response of the mesosphere-thermosphere-ionosphere system to global change – CAWSES-II contribution	22
The geospace response to variable inputs from the lower atmosphere: A review of the progress made by Task Group 4 of CAWSES-II	23

2. Atmospheric and hydrospheric sciences

Marine microplastics as vectors of major ocean pollutants and its hazards to the marine ecosystem and humans	26
Applications of soft computing models for predicting sea surface temperature: a comprehensive review and assessment	27
Two decades of Earth system modeling with an emphasis on Model for Interdisciplinary Research on Climate (MIROC)	28
d4PDF: large-ensemble and high-resolution climate simulations for global warming risk assessment	29

DYAMOND: The DYNAMics of the Atmospheric general circulation Modeled On Non-hydrostatic Domains ...	30
Toward reduction of the uncertainties in climate sensitivity due to cloud processes using a global non-hydrostatic atmospheric model	31
Maritime continent coastlines controlling Earth's climate	32
Outcomes and challenges of global high-resolution non-hydrostatic atmospheric simulations using the K computer	33
A review of atmospheric chemistry observation at mountain sites	34
A review of progress towards understanding the transient global mean surface temperature response to radiative perturbation	35
Overview of the development of the Aerosol Loading Interface for Cloud microphysics In Simulation (ALICIS)	36
The dynamics of the mesosphere and lower thermosphere: a brief review	37
Modeling in Earth system science up to and beyond IPCC AR5	38
The Non-hydrostatic Icosahedral Atmospheric Model: Description and Development	39

3. Human geosciences • Biogeosciences

Arsenic cycling in the Earth's crust and hydrosphere: interaction between naturally occurring arsenic and human activities	42
Perspective on the response of marine calcifiers to global warming and ocean acidification – Behavior of corals and foraminifera in a high CO ₂ world “hot house”	43
Theoretical constraints of physical and chemical properties of hydrothermal fluids on variations in chemolithotrophic microbial communities in seafloor hydrothermal systems.	44
Biochemical and physiological bases for the use of carbon and nitrogen isotopes in environmental and ecological studies	45

4. Solid earth sciences

Visualizing heterogeneities of earthquake hypocenter catalogs: modeling, analysis, and compensation	48
Strength models of the terrestrial planets and implications for their lithospheric structure and evolution	49
Deep mantle melting, global water circulation and its implications for the stability of the ocean mass	50
A coupled core-mantle evolution: Review and future prospects	51
Some remarks on hydrogen-assisted electrical conductivity in olivine and other minerals	52
Detection of repeating earthquakes and their application in characterizing slow fault slip	53
Nitrogen in the Earth: abundance and transport	54
Earthquake Early Warning: what does “seconds before a strong hit” mean?	55
Redox-controlled mechanisms of C and H isotope fractionation between silicate melt and COH fluid in the Earth's interior	56
Nonlinear dynamical analysis of GNSS data: quantification, precursors and synchronization	57
Structural context and variation of ocean plate stratigraphy, Franciscan Complex, California: insight into mélange origins and subduction-accretion processes	58
Seismic imaging of slab metamorphism and genesis of intermediate-depth intraslab earthquakes	59
Imaging in 3D under pressure: a decade of high-pressure X-ray microtomography development at GSECARS	60
Philippine Sea Plate inception, evolution and consumption with special emphasis on the early stages of Izu-Bonin-Mariana subduction	61
Mantle hydration and Cl-rich fluids in the subduction forearc	62

Iron snow, crystal floats, and inner-core growth: modes of core solidification and implications for dynamos in terrestrial planets and moons	63
Liquid Sodium Models of the Earth's Core	64
Towards more realistic core-mantle boundary heat flux patterns: a source of diversity in planetary dynamos	65
Sound velocity of hcp-Fe at high pressure: experimental constraints, extrapolations and comparison with seismic models	66
Earthquake faulting in subduction zones: insights from fault rocks in accretionary prisms	67
Water-melt interaction in hydrous magmatic systems at high temperature and pressure	68

5. Interdisciplinary research

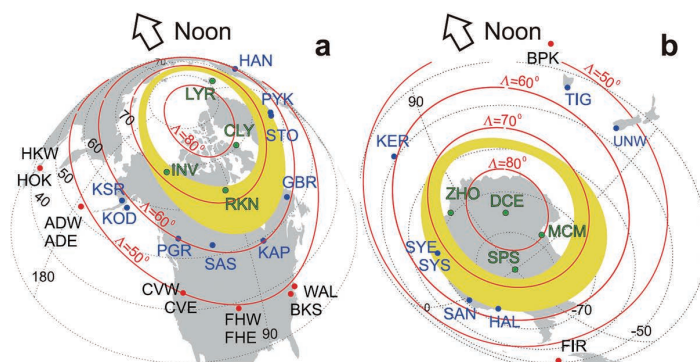
Coupling library Jcup3: its philosophy and application	70
Morphometric measurements of bedrock rivers at different spatial scales and applications to geomorphological heritage research	71
Northern Eurasia Future Initiative (NEFI): facing the challenges and pathways of global change in the twenty-first century	72
Cenozoic sedimentary records of climate-tectonic coupling in the Western Himalaya	73
Transitional changes in microfossil assemblages in the Japan Sea from the Late Pliocene to Early Pleistocene related to global climatic and local tectonic events	74
Evolution and variability of the Asian monsoon and its potential linkage with uplift of the Himalaya and Tibetan Plateau	75
Geochemical approaches to the quantification of dispersed volcanic ash in marine sediment	76
Sea surface temperature proxies (alkenones, foraminiferal Mg/Ca, and planktonic foraminiferal assemblage) and their implications in the Okinawa Trough	77
Marine tephra in the Japan Sea sediments as a tool for paleoceanography and paleoclimatology	78
The Pliocene to Recent History of the Kuroshio and Tsushima Currents: a multi-proxy approach	79

Review of the accomplishments of Mid-latitude Super Dual Auroral Radar Network (SuperDARN) HF Radars

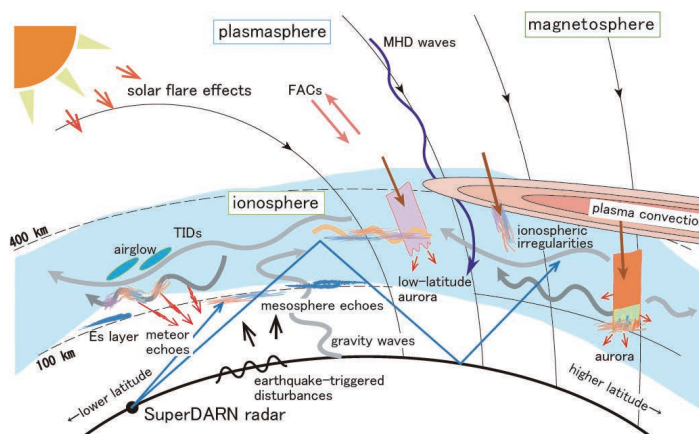
Nishitani N, Ruohoniemi JM, Lester M, Baker JBH, Koustov AV, Shepherd SG, Chisham G, Hori T, Thomas EG, Makarevich RA, Marchaudon A, Ponomarenko P, Wild JA, Milan SE, Bristow WA, Devlin J, Miller E, Greenwald RA, Ogawa T, Kikuchi T

[Keywords] Mid-latitude SuperDARN, Ionosphere, Magnetosphere, Convection, Ionospheric irregularities, HF propagation analysis, Ion-neutral interactions, MHD waves

The Super Dual Auroral Radar Network (SuperDARN) is a network of high-frequency (HF) radars located in the high- and mid-latitude regions of both hemispheres that is operated under international cooperation. The network was originally designed for monitoring the dynamics of the ionosphere and upper atmosphere in the high-latitude regions. However, over the last approximately 15 years, SuperDARN has expanded into the mid-latitude regions. With radar coverage that now extends continuously from auroral to sub-auroral and mid-latitudes, a wide variety of new scientific findings have been obtained. In this paper, the background of mid-latitude SuperDARN is presented at first. Then, the accomplishments made with mid-latitude SuperDARN radars are reviewed in five specified scientific and technical areas: convection, ionospheric irregularities, HF propagation analysis, ion-neutral interactions, and magnetohydrodynamic (MHD) waves. Finally, the present status of mid-latitude SuperDARN is updated and directions for future research are discussed.



Schematic plots showing the a Northern and b Southern Hemisphere SuperDARN radar locations with respect to the auroral oval. The model auroral oval (yellow) for moderately disturbed conditions is plotted with the SuperDARN radar locations identified in green type and green closed circles (polar cap latitudes), blue type and blue closed circles (auroral latitudes), and black type and red closed circles (mid-latitude radars).



Schematic illustration of natural phenomena which can be studied by SuperDARN radars.

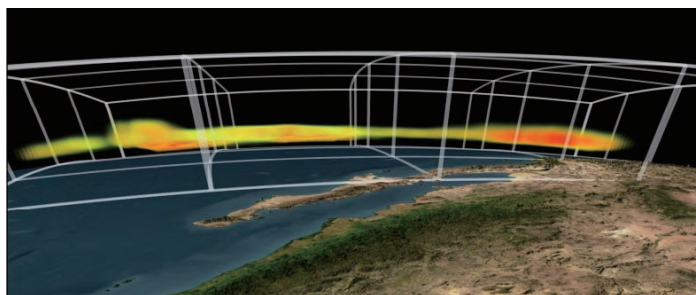


The science case for the EISCAT_3D radar

McCrea I, Aikio A, Alfonsi L, Belova E, Buchert S, Clilverd M, Engler N, Gustavsson B, Heinselman C, Kero J, Kosch M, Lamy H, Leyser T, Ogawa Y, Oksavik K, Pellinen-Wannberg A, Pitout F, Rapp M, Stanislawski I, Vierinen J

[Keywords] EISCAT, EISCAT_3D, Radar, Incoherent scatter, Atmospheric science, Space physics, Plasma physics, Solar system research, Space weather, Radar techniques

The EISCAT (European Incoherent SCATer) Scientific Association has provided versatile incoherent scatter (IS) radar facilities on the mainland of northern Scandinavia (the EISCAT UHF and VHF radar systems) and on Svalbard (the electronically scanning radar ESR (EISCAT Svalbard Radar) for studies of the high-latitude ionised upper atmosphere (the ionosphere). The mainland radars were constructed about 30 years ago, based on technological solutions of that time. The science drivers of today, how-



Schematic representation showing the volumetric imaging of an ionospheric layer above Scandinavia by EISCAT_3D. (Image courtesy of EISCAT Scientific Association)

ever, require a more flexible instrument, which allows measurements to be made from the troposphere to the topside ionosphere and gives the measured parameters in three dimensions, not just along a single radar beam. The possibility for continuous operation is also an essential feature. To facilitate future science work with a world-leading IS radar facility, planning of a new radar system started first with an EU-funded Design Study (2005–2009) and has continued with a follow-up EU FP7 EISCAT_3D Preparatory Phase project (2010–2014). The radar facility will be realised by using phased arrays, and a key aspect is the use of advanced software and data processing techniques. This type of software radar will act as a pathfinder for other facilities worldwide. The new radar facility will enable the EISCAT_3D science community to address new, significant science questions as well as to serve society, which is increasingly dependent on space-based technology and issues related to space weather. The location of the radar within the auroral oval and at the edge of the stratospheric polar vortex is also ideal for studies of the long-term variability in the atmosphere and global change. This paper is a summary of the EISCAT_3D science case, which was prepared as part of the EU-funded Preparatory Phase project for the new facility. Three science working groups, drawn from the EISCAT user community, participated in preparing this document. In addition to these working group members, who are listed as authors, thanks are due to many others in the EISCAT scientific community for useful contributions, discussions, and support.

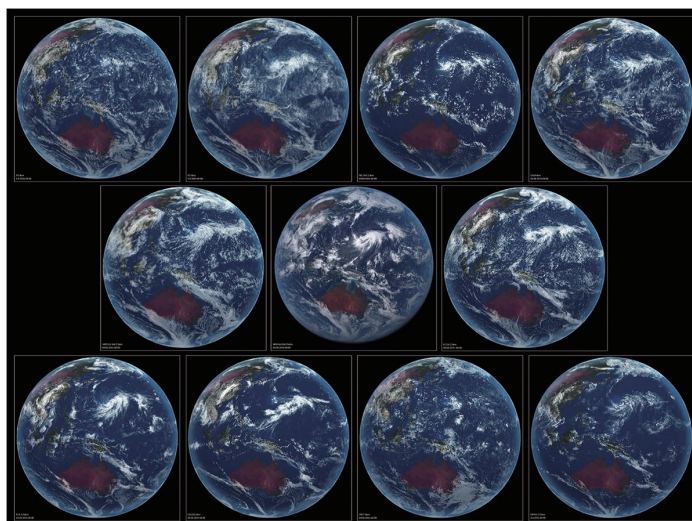


DYAMOND: The DYnamics of the Atmospheric general circulation Modeled On Non-hydrostatic Domains

Stevens B, Satoh M, Auger L, Biercamp J, Bretherton CS, Chen X, Duben P, Judt F, Khairoutdinov M, Klocke D, Kodama C, Kornblueh L, Lin SJ, Neumann P, Putman WM, Rober N, Shibuya R, Vanniere B, Vidale PL, Wedi N, Zhou L

[Keywords] Climate modelling, Model intercomparison project, Tropical Convection

A review of the experimental protocol and motivation for DYAMOND, the first intercomparison project of global storm-resolving models, is presented. Nine models submitted simulation output for a 40-day (1 August–10 September 2016) intercomparison period. Eight of these employed a tiling of the sphere that was uniformly less than 5 km. By resolving the transient dynamics of convective storms in the tropics, global storm-resolving models remove the need to parameterize tropical deep convection, providing a fundamentally more sound representation of the climate system and a more natural link to commensurately high-resolution data from satellite-borne sensors. The models and some basic characteristics of their output are described in more detail, as is the availability and planned use of this output for future scientific study. Tropically and zonally averaged energy budgets, precipitable water distributions, and precipitation from the model ensemble are evaluated, as is their representation of tropical cyclones and the predictability of column water vapor, the latter being important for tropical weather.



Snapshot of DYAMOND Models. Shown is a snapshot of the models taken from the perspective of the Himawari-8. The images are for the cloud scene on 4 August 2016, and are qualitatively rendered based on each model's condensate fields to illustrate the variety of convective structures resolved by the models, and difficulty of distinguishing them from actual observations. From left to right, the images are from IFS-4km, IFS-9km, NICAM, and SAM (top row); Arpege, Himawari, and ICON (middle row); FV3, GEOS5, UKMO and MPAS (bottom row).



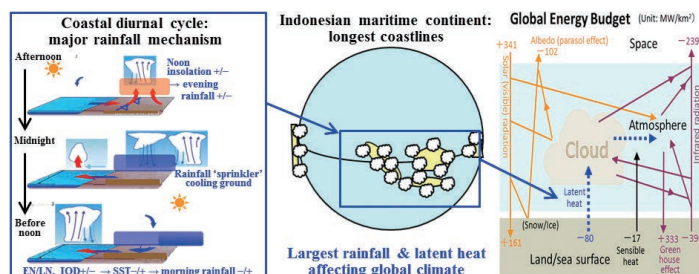
Maritime continent coastlines controlling Earth's climate

Yamanaka MD, Ogino SY, Wu PM, Hamada JI, Mori S, Matsumoto J, Syamsudin F

[Keywords] Indonesian maritime continent, Atmosphere–ocean–land interaction, Convective clouds, Multiple scales, Diurnal cycle, Sea–land breeze circulation

During the Monsoon Asian Hydro–Atmosphere Scientific Research and Prediction Initiative (MAHASRI; 2006–16), we carried out two projects over the Indonesian maritime continent (IMC), constructing the Hydrometeorological Array for Intraseasonal Variation–Monsoon Automonitoring (HARIMAU; 2005–10) radar network and setting up a prototype institute for climate studies, the Maritime Continent Center of Excellence (MCCOE; 2009–14). Here, we

review the climatological features of the world's largest “regional” rainfall over the IMC studied in these projects. The fundamental mode of atmospheric variability over the IMC is the diurnal cycle generated along coastlines by land–sea temperature contrast: afternoon land becomes hotter than sea by clear-sky insolation before noon, with the opposite contrast before sunrise caused by evening rainfall-induced “sprinkler”-like land cooling (different from the extratropical infrared cooling on clear nights). Thus, unlike the extratropics, the diurnal cycle over the IMC is more important in the rainy season. The intraseasonal, seasonal to annual, and interannual climate variabilities appear as amplitude modulations of the diurnal cycle. For example, in Jawa and Bali the rainy season is the southern hemispheric summer, because land heating in the clear morning and water vapor transport by afternoon sea breeze is strongest in the season of maximum insolation. During El Niño, cooler sea water surrounding the IMC makes morning maritime convection and rainfall weaker than normal. Because the diurnal cycle is almost the only mechanism generating convective clouds systematically near the equator with little cyclone activity, the local annual rainfall amount in the tropics is a steeply decreasing function of coastal distance (e-folding scale 100–300 km), and regional annual rainfall is an increasing function of “coastline density” (coastal length/land area) measured at a horizontal resolution of 100 km. The coastline density effect explains why rainfall and latent heating over the IMC are twice the global mean for an area that makes up only 4% of the Earth's surface. The diurnal cycles appearing almost synchronously over the whole IMC generate teleconnections between the IMC convection and the global climate. Thus, high-resolution (<100 km; <1 day) observations and models over the IMC are essential to improve both local disaster prevention and global climate prediction.



Maritime–continental diurnal-cycle rain and latent heat controlling global climate

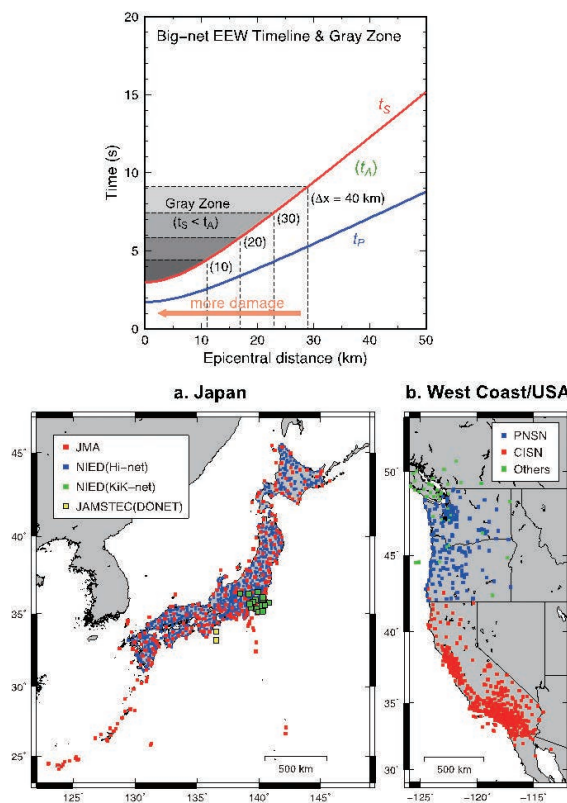


Earthquake Early Warning: what does “seconds before a strong hit” mean?

Tajima F, Hayashida T.

[Keywords] Earthquake early warning, effective preparation for seismic safety at recipients' sites, short-wavelength ground motion variation

An earthquake early warning (EEW) system is designed to detect an event, determine its parameters (hypocenter, magnitude, and origin time), and issue an alert to sites/areas where necessary actions should be taken before destructive seismic energy arrivals. At present, large-scale EEW systems are operational in several countries around the world. The most extensive nationwide EEW system has been operating in Japan since 2007, and was able to issue alerts broadly when the moment magnitude (M_w) 9 Tohoku-Oki earthquake hit in 2011. The casualties caused by this event were far less than those caused by other deadly earthquakes ($M_w \geq 6.6$) in this century. Many other countries attributed the fewer death victims to the advanced large-scale EEW system, and plan to install systems similar to Japan's model. However, the historical and environmental background in Japan, both in terms of earthquake hazards and safety preparation, differs considerably from other countries. In addition, EEW systems that use data from a large-scale network (i.e., “a big-net” hereafter) still have limitations. There are thus numerous factors that other countries should consider to benefit from installing a Japan-styled EEW. In this article, we review how research and development associated with EEW have been carried out, and how EEW systems presently function. We then show short-wavelength variation of ground motions within the typical station interval of a big-net using data recorded by a dense local seismic network in Japan. However, it is not particularly meaningful to attempt detailed modeling of varieties of ground motion within the station interval for a big-net EEW operation, because the possible combinations of earthquake sources, paths of wave propagation, and recipient sites are infinite. We emphasize that in all circumstances, for recipients to benefit from EEW, seismic safety preparations must be implemented. Necessary preparations at sites do not diminish in importance after incremental improvements in station coverage and/or algorithms in a big-net operation. Further, scientists and engineers involved in EEW projects should strive to publically disseminate how big-net EEW systems work, and also why, to achieve maximum benefit, these systems should always be supplemented by preparations at recipients' sites.



(top)

Big-net timeline of EEW alert issuance at t_A and gray zones where strong shaking may arrive at t_s before t_A . The vertical axis is the time relative to an earthquake origin time, and the horizontal axis the epicentral distance (D). Gray zones are illustrated for networks of different station spacing $\Delta x = 10, 20, 30$, and 40 km. For example, for a network of $\Delta x = 20$ km, the gray zone radius is ~ 17 km from the epicenter, where the ground shaking may arrive before an alert and is likely to be stronger, causing more damage than outside of it.

(bottom)

Big-net station distributions: a. the station spacing in Japan is ~ 20 km or less over the country. This implies that the average gray zone radius is ~ 17 km from a hypocenter; b. the station spacing in the West Coast/USA is not homogeneous, i.e., it is ~ 10 km in the populated metropolitan areas such as around Los Angeles, San Francisco Bay and Seattle whereas it is larger in less populated areas.

Published: 2018/10/10

<https://doi.org/10.1186/s40645-018-0221-6>



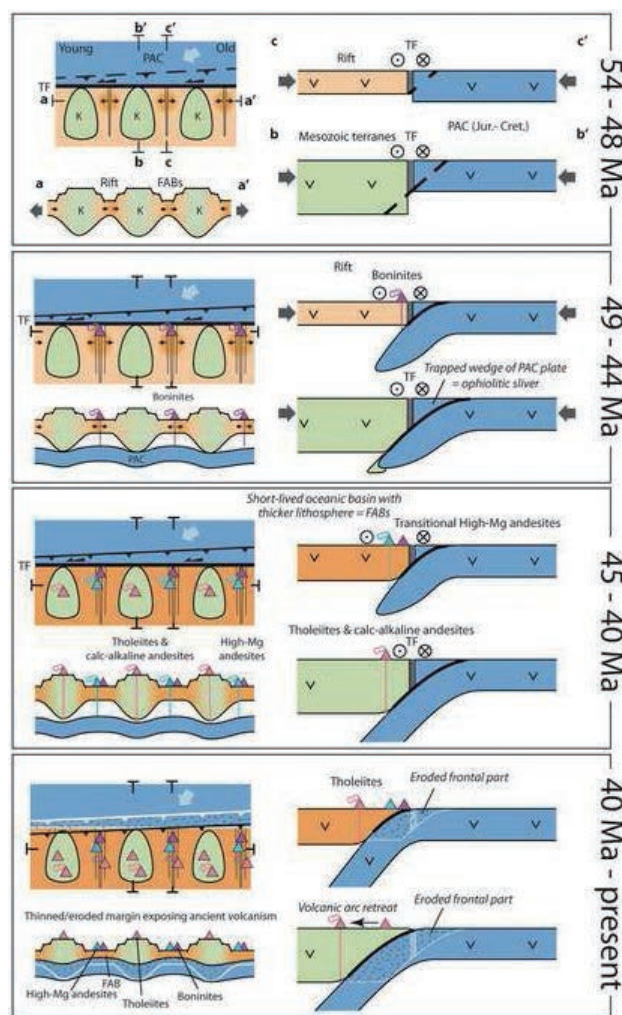
Philippine Sea Plate inception, evolution and consumption with special emphasis on the early stages of Izu-Bonin-Mariana subduction

Lallemant S

[Keywords] Philippine Sea Plate, Izu-Bonin-Mariana, subduction initiation, boninite, fore-arc basalt, serpentinite mud volcano, back-arc basin, transform fault, arc terrane, plume-ridge interaction

We compiled the most relevant data acquired throughout the Philippine Sea Plate (PSP) from the early expeditions to the most recent. We also analyzed the various explanatory models in light of this updated dataset. The following main conclusions are discussed in this study.

(1) The Izanagi slab detachment beneath the East Asia margin around 60–55 Ma likely triggered the Oki-Daito plume occurrence, Mesozoic proto-PSP splitting, shortening and then failure across the paleo-transform boundary between the proto-PSP and the Pacific Plate, Izu-Bonin-Mariana subduction initiation and ultimately PSP inception. (2) The initial splitting phase of the composite proto-PSP under the plume influence at ~54–48 Ma led to the formation of the long-lived West Philippine Basin and short-lived oceanic basins, part of whose crust has been ambiguously called “fore-arc basalts” (FABs). (3) Shortening across the paleo-transform boundary evolved into thrusting within the Pacific Plate at ~52–50 Ma, allowing it to subduct beneath the newly formed PSP, which was composed of an alternance of thick Mesozoic terranes and thin oceanic lithosphere. (4) The first magmas rising from the shallow mantle corner, after being hydrated by the subducting Pacific crust beneath the young oceanic crust near the upper plate spreading centers at ~49–48 Ma were boninites. Both the so-called FABs and the boninites formed at a significant distance from the incipient trench, not in a fore-arc position as previously claimed. The magmas erupted for 15 m.y. in some places, probably near the intersections between back-arc spreading centers and the arc. (5) As the Pacific crust reached greater depths and the oceanic basins cooled and thickened at ~44–45 Ma, the composition of the lavas evolved into high-Mg andesites and then arc tholeiites and calc-alkaline andesites. (6) Tectonic erosion processes removed about 150–200 km of frontal margin during the Neogene, consuming most or all of the Pacific ophiolite initially accreted to the PSP. The result was exposure of the FABs, boninites, and early volcanics that are near the trench today. (7) Serpentinite mud volcanoes observed in the Mariana fore-arc may have formed above the remnants of the paleo-transform boundary between the proto-PSP and the Pacific Plate.



Schematic tectono-magmatic model of IBM subduction initiation and early evolution. Special emphasis has been done on the geodynamic context of various magma1 eruptions. The white lines in stage “40 Ma - present” represent the former positions of plate boundaries or the base of the upper plate in stage “45-40 Ma”.

TF = transform fault, PAC = Pacific, FAB = Forearc basalts

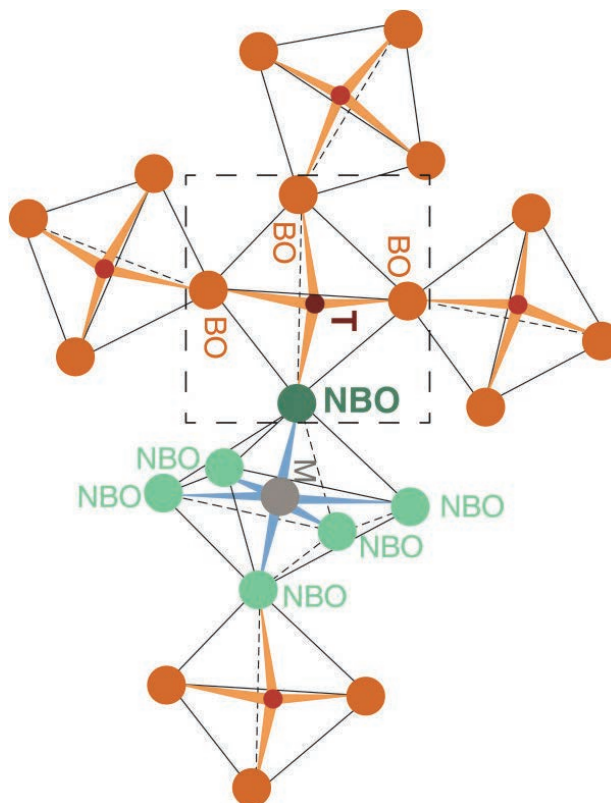


Water-melt interaction in hydrous magmatic systems at high temperature and pressure

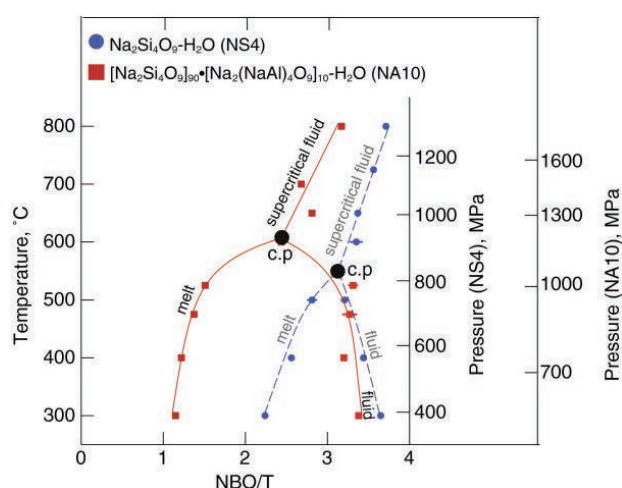
Bjorn Mysen

[Keywords] Hydrous magma, Aqueous fluid, Melt structure, Viscosity, Isotope partitioning, Partial melting, Water solubility, Silicate solubility, Glass transition, Solution mechanism

Experimental data on the structure and properties of melts and fluids relevant to water-melt interaction in hydrous magmatic systems in the Earth's interior have been reviewed. Complex relationships between water solubility in melts and their bulk composition [Al/Si-ratio, metal oxide/(Al + Si) and electron properties of metal cations] explain why water solubility in felsic magmas such as those of rhyolite and andesite composition is significantly greater than the water solubility in basalt melts. The silicate solubility in aqueous fluid is also significantly dependent on composition with metal oxide/(Al + Si) and electron properties of the metal cations, the dominant variables. Hydrogen bonding is not important in hydrous fluids and melts at temperatures above 500°C to 550°C and does not, therefore, play a role in hydrous magmatic systems. The properties of hydrous melts and aqueous solutions are governed by how the silicate speciation (Q^n species, where n is the number of bridging oxygen in an individual species) varies with bulk composition, silicate composition, temperature, and pressure. The reactions that describe the interactions are similar in melts, fluids, and supercritical fluids. The degree of melt polymerization caused by dissolved water varies with melt composition and total water content. Silicate- and alkali-rich felsic magmatic melts are more sensitive to water content than more mafic magmas. Transport and configurational properties of hydrous magmatic melts can be modeled with the aid of the Q^n speciation variations. Liquidus and melting phase relations of hydrous systems also can be described in such terms, as can minor and trace element partition coefficients. Stable isotope fractionation (e.g., D/H) can also be rationalized in this manner. Critical to these latter observations is the high silicate concentration in aqueous fluids. These components can enhance solubility of minor and trace elements by orders of magnitude and change the speciation of H and D complexes so that their fractionation factors change quite significantly. Data from pure silicate-H₂O systems cannot be employed for these purposes.



Schematic representation of the concept of bridging (BO) and nonbridging (NBO) oxygen



Degree of silicate polymerization, NBO/T. In silicate in hydrous melts, silicate-saturated aqueous fluid, and supercritical fluid in a hydrous Na-aluminosilicate system

Published: 2014/4/22

<https://doi.org/10.1186/2197-4284-1-4>

Review

Interdisciplinary research

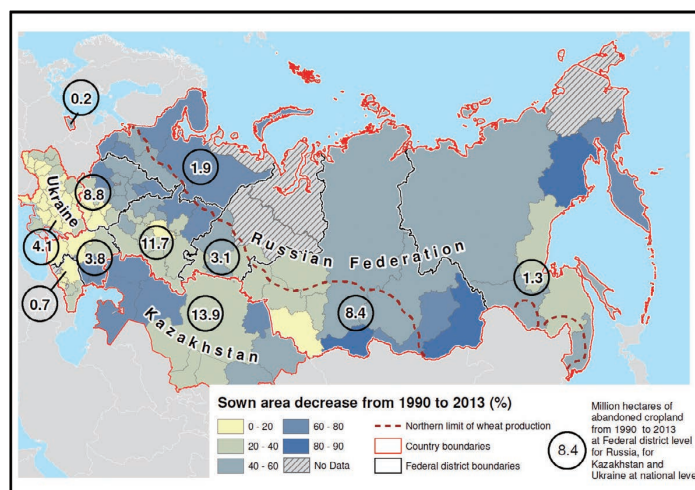
Northern Eurasia Future Initiative (NEFI): facing the challenges and pathways of global change in the twenty-first century

Pavel Groisman et al.

[Keywords] Environmental Changes, Northern Eurasia, Ecosystems dynamics, Terrestrial water cycle, Cryosphere retreat, Extreme and inclement environmental conditions, Sustainable development, Land-cover and land-use change, Integrated assessment models for decision-makers

During the past several decades, the Earth system has changed significantly, especially across Northern Eurasia. Changes in the socio-economic conditions of the larger countries in the region have also resulted in a variety of regional environmental changes that can have global consequences. The Northern Eurasia Future Initiative (NEFI) has been designed as an essential continuation of the Northern Eurasia Earth Science Partnership Initiative (NEESPI), which was launched in 2004. NEESPI sought to elucidate all aspects of ongoing environmental change, to inform societies and, thus, to better prepare societies for future developments. A key principle of NEFI is that these developments must now be secured through science-based strategies co-designed

with regional decision-makers to lead their societies to prosperity in the face of environmental and institutional challenges. NEESPI scientific research, data, and models have created a solid knowledge base to support the NEFI program. This paper presents the NEFI research vision consensus based on that knowledge. It provides the reader with samples of recent accomplishments in regional studies and formulates new NEFI science questions. To address these questions, nine research foci are identified and their selections are briefly justified. These foci include warming of the Arctic; changing frequency, pattern, and intensity of extreme and inclement environmental conditions; retreat of the cryosphere; changes in terrestrial water cycles; changes in the biosphere; pressures on land use; changes in infrastructure; societal actions in response to environmental change; and quantification of Northern Eurasia's role in the global Earth system. Powerful feedbacks between the Earth and human systems in Northern Eurasia (e.g., mega-fires, droughts, depletion of the cryosphere essential for water supply, retreat of sea ice) result from past and current human activities (e.g., large-scale water withdrawals, land use, and governance change) and potentially restrict or provide new opportunities for future human activities. Therefore, we propose that integrated assessment models are needed as the final stage of global change assessment. The overarching goal of this NEFI modeling effort will enable evaluation of economic decisions in response to changing environmental conditions and justification of mitigation and adaptation efforts.



Changes in sown areas across the former Soviet Union (Russia, Ukraine, and Kazakhstan) from 1990 to 2013. Areas of abandoned sown areas for this period are 40 Mha in Russia (Rosstat 2016), 5.4 Mha in Ukraine (Ukrstat 2014), and 13 Mha in Kazakhstan (Kazstat 2014).

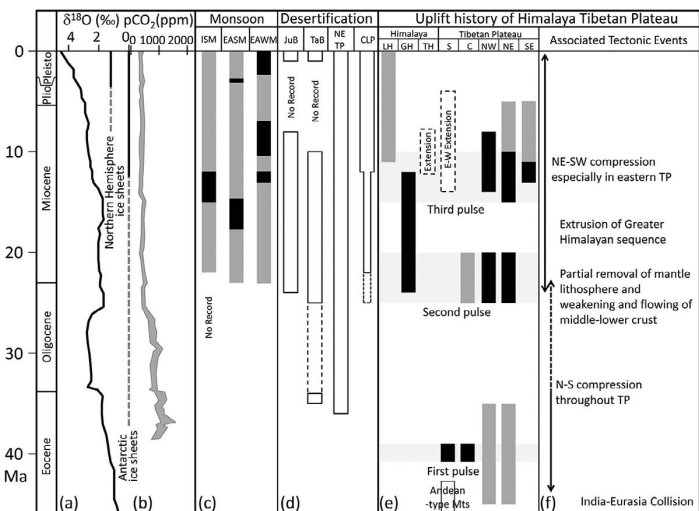


Evolution and variability of the Asian monsoon and its potential linkage with uplift of the Himalaya and Tibetan Plateau

Tada R, Zheng H, Cliff P D

[Keywords] East Asian summer monsoon, East Asian winter monsoon, Indian summer monsoon, Himalaya, Tibetan Plateau, Chinese Loess Plateau, Climate model, Tectonic–climate linkage, Westerly jet, Desertification

In the densely populated region of East Asia, it is important to know the mechanism, scale, and frequency of heavy precipitation brought about during the monsoons and typhoons. However, observational data, which cover only several decades, are insufficient to examine the long-term trend of extreme precipitation and its background mechanism. In humid areas, the transport flux of a suspended detrital material through a river system is known to have an empirical power relationship with precipitation. Thus, the sedimentation flux of a fine detrital material could potentially be used as a proxy for reconstructing past heavy precipitation events. To test the idea that the sedimentation flux of detrital materials records past heavy precipitation events (e.g., typhoons), we focused on the detrital flux estimated from the annually laminated sediment of Lake Suigetsu, central Japan, which is capable of accurately correlating the age of detrital flux with the precipitation record. We first established a precise age model (error within ± 1 year in average) beginning in 1920 A.D. on the basis of varve counting fine-tuned by correlation between event layers with historical floods. The flux of the detrital material ($\text{g}/\text{cm}^2/\text{year}$) was estimated on the basis of Al_2O_3 content (wt%), dry bulk density (g/cm^3), and sedimentation rate (cm/year) calculated from the age model. The detrital flux of background sedimentation showed a weak positive correlation with annual and monthly (June and September) precipitation excluding heavy precipitation that exceeded 100 mm/day. Furthermore, the thickness of instantaneous event layers, which corresponds to several maxima of detrital flux and is correlated with floods that occurred mainly during typhoons, showed a positive relationship with the total amount of precipitation that caused a flood event. This result suggests that the detrital flux maxima (deposition of event layers) record past extreme precipitation events that were likely associated with typhoons that hit the middle part of Honshu Island. Based on this result, the record of typhoon-caused flood events can go back to older period (e.g., last glacial period) on the basis of the occurrence, and thickness, or mass flux of event layers using long sediment cores from Lake Suigetsu.



Evolution of Asian monsoons, desertification, HTP uplift, and their relation with global changes during Cenozoic. Temporal changes of a $\delta^{18}\text{O}$ of benthic foraminifera (modified from Zachos et al. 2001) and b pCO_2 (modified from Zhang et al. 2013) are compared with temporal evolution of c Asian monsoons, d desertification, e HTP uplift, and f associated tectonic events. In c and e, gray bars represent weak phases and black bars represent strong phases. In d, JuB and TaB indicate Jungger Basin and Tarim Basin, respectively.

